RASĀYAN *J. Chem.*
Vol. 18 | No. 4 | 2263-2274 | October-December | 2025
ISSN: 0974-1496 | e-ISSN: 0976-0083 | CODEN: RJCABP
http://www.rasayanjournal.com
http://www.rasayanjournal.co.in

PHOTOCATALYTIC DEGRADATION AND BIOLOGICAL STUDIES OF NOVEL SCHIFF BASE 5-CHLORO-*N*-[(1*Z*)-1*H*-INDOL-3-YLMETHYLENE]PYRIDIN-2-AMINE AND ITS Co(II), Ni(II) AND Cu(II) COMPLEXES

G.Y. Akarsh[1], H.A. Anilkumara[1], N.K. Vasantakumarnaik[1], N. Ranjitha[1], G. Suma[1], K.M. Pooja[2] and G. Krishnamurthy[1,✉]

[1]Department of P.G. Studies and Research in Chemistry and Industrial Chemistry, Sahyadri Science College, Kuvempu University, Shivamogga-577203, Karnataka, India

[2]Department of P.G. Studies and Research in Chemistry, Sahyadri Science College, Kuvempu University, Shivamogga-577203, Karnataka, India

✉Corresponding author: gkmnaiksahyadri@gmail.com

ABSTRACT

The present work highlights the synthesis of a novel Schiff base ligand, 5-chloro-*N*-[(1*Z*)-1*H*-indol-3-ylmethylene]pyridin-2-amine (CIA) and its metal complexes. The structure of the synthesized compounds has been evaluated using various physicochemical and spectroscopic techniques. The biological investigation of the synthesized ligand and its metal complexes has been determined against the bacteria (*Staphylococcus aureus* and *Escherichia coli*) and fungal (*A. flavus* and *P. anomala*), indicating that the metal complexes have greater effectiveness than the uncoordinated ligand among the synthesized metal complexes, the $[Cu(CIA)_2Cl_2]$ complex exhibiting notable efficacy against bacterial and fungal strains. Antioxidant activity using the DPPH standard method is measured through IC_{50} values, which show promising biological activity by all the synthesized compounds. In addition, the photodegradation of Eriochrome Black T dye was investigated under visible light in the presence of the metal complexes to assess their catalytic efficiency. Spectral analysis reveals photodegradation percentages of 31.81%, 35.29% and 67.44% for Co(II), Ni(II), and Cu(II) complexes, respectively. The results revealed that the $[Cu(CIA)_2Cl_2]$ exhibited superior performance when compared to the other complexes.

Keywords: Schiff Base, Metal Complexes, Photocatalytic, Antimicrobial, Antioxidant.

RASĀYAN *J. Chem.*, Vol. 18, No.4, 2025

INTRODUCTION

Schiff base is a compound with the functional group $R_1CH=NR_2$, where R_1 and R_2 are organic groups or hydrogen atoms. These bases result from condensation reactions between primary amines and carbonyl compounds like aldehydes or ketones.[1-4] Schiff bases are widely studied for their applications in coordination chemistry and their diverse roles in organic synthesis, catalysis, and medicinal chemistry.[5-8] The term Schiff is derived from its inventor, Hugo Schiff, who initially described its synthesis in the 1860s. Schiff base metal complexes are coordination compounds formed by the reaction of a metal ion with a Schiff base ligand. The coordination modes of Schiff base ligands vary from mono-dentate to poly-dentate, depending on the number of donor atoms present in the ligand. Schiff base metal complexes exhibit a wide range of properties and applications. In catalysis, they are used as catalysts for various organic reactions such as hydrogenation, oxidation, and cycloaddition reactions. Derivatives of Schiff base and their metal complexes display antimicrobial and antioxidant properties.[9-14] In material science, they are used in the development of electronic and magnetic materials. Further, Schiff bases and their derivatives are used in sensor technology in the detection of metal ions.[15-17] To summarize, unique structural and electronic properties of Schiff base derivatives and their metal complexes make them highly adaptable compounds with a broad range of applications in various fields such as chemistry, biology, and materials science. In view of the above, a few Schiff base derivatives and their metal complexes have been synthesized in our laboratory, and the results of biological activities and

http://doi.org/10.31788/RJC.2025.1849359

photocatalytic properties were reported.[18-20] In continuation of the previous work, we report here the synthesis of a novel Schiff base ligand 5-chloro-*N*-[(1*Z*)-1*H*-indol-3-ylmethylene]pyridin-2-amine (CIA), and its transition metal complexes. The synthesized compounds were found to have excellent antimicrobial, antioxidant, and photocatalytic properties.

EXPERIMENTAL

Material and Methods

The synthesis of the ligand utilized Indole-3-carboxaldehyde, 2-Amino-5-chloropyridine, and acetic acid, produced from Sd-fine chemicals. Ethanol was purified according to established literature.[21] Laboratory-grade metal salts were obtained from Sigma Aldrich and used without purification. The melting point was determined using the Innovative DTC-967A apparatus. The amount of carbon, hydrogen, and nitrogen was determined using the Perkin-Elmer 2400 series II analyzer. The synthesized compounds were characterized using various analytical techniques. FTIR Spectroscopy recorded in 350-4000 cm^{-1} using IR-Spirit Shimadzu serial no: A224159 (Made in Japan) was utilized to obtain IR Spectra at Sahyadri Science College, Shivamogga-577203, Karnataka, India. The absorption spectra were recorded using a Systronics UV-Vis Double Beam Spectrophotometer 2206TS at Sahyadri Science College, Shivamogga-577203, Karnataka, India. The ^1H NMR spectra were analyzed using a JEOL spectrometer operating at 400 MHz at Mangalore University, Mangalore-574199, Karnataka, India. The LC-MS analysis was performed using an MS Make (Made in USA) UPLC at Mysore - 570001, Karnataka, India. The XRD composition was analyzed using a Bruker D8 Advance, and the SEM analysis was performed using a Zeiss modelEVO LS 15.

General Procedure

Synthesis of Schiff Base Ligand

The novel Schiff base ligand, 5-chloro-*N*-[(1*Z*)-1*H*-indol-3-ylmethylene]pyridin-2-amine (CIA) was synthesized by following the literature procedure with little modifications. Here, equimolar ratios of Indole-3-carboxaldehyde (0.002 mol) and 2-Amino-5-chloropyridine (0.002 mol) were taken in a round-bottomed flask and dissolved in ethanol (20 mL). To the above solution, 5-6 drops of acetic acid are added as a catalyst. The solution was kept for reflux on a water bath for 4 hrs, and the progress of the reaction was monitored by TLC. After completion of the reaction, the solution was transferred to a petri dish and allowed to dry. The precipitate formed was filtered, recrystallized with ethanol, and dried in air.

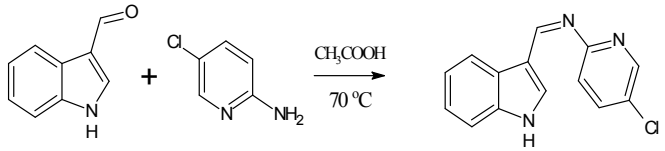

Scheme-1: Synthetic path of 5-chloro-*N*-[(1*Z*)-1*H*-indol-3-ylmethylene]pyridin-2-amine (CIA)

General Procedure for the Synthesis of Metal Complexes

The synthesized ligand (CIA) (0.002 mol) was taken in a round-bottomed flask and dissolved in 10 mL of absolute ethanol. Chlorides of each metal (Co, Ni, and Cu) (0.001 mol) were dissolved separately in absolute ethanol and transferred to the ligand solution. The obtained solutions were stirred and refluxed for 4-5 hrs on a water bath. Excess solvent was removed by evaporation to get the solid product. The obtained product was allowed to cool at ambient temperature. The precipitate was filtered, washed, and dried. The synthetic pathway and the probable structure of the metal complexes are shown in Scheme-2.

Photocatalytic Activity

The photocatalytic performance was evaluated by assessing the degradation of Eriochrome black T (EBT) with a catalytic amount of the synthesized metal complexes under sunlight. Initially, 50 mg photocatalyst was dispersed thoroughly in 100 mL aqueous solution of EBT. To establish

absorption and desorption equilibrium between EBT and photocatalyst, the solution was magnetically stirred in the dark for 15 minutes before irradiation. From the above solution, 3 mL aliquots were collected at predetermined time intervals, and by centrifugation removed the particles. The concentration of EBT was quantified by measuring the absorbance at the characteristic wavelength using a Systronics UV-Vis double beam spectrophotometer 2206TS.

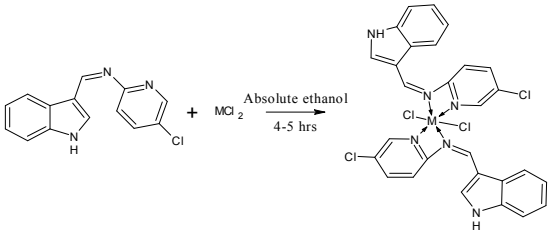

M = Co^{+2}, Ni^{+2} and Cu^{+2}

Scheme-2: Synthetic Method and Structure of the Metal Complexes

Antimicrobial Activities

Antimicrobial activity of the samples was evaluated using the agar diffusion method, as described by the standard procedure with slight modifications.[22,23] The bacterial strains *Staphylococcus aureus* MTCC-7443 (Gram-positive), *Escherichia coli* MTCC-7410 (Gram-negative). The fungal species *Aspergillus flavus* MTCC-9606 and *Pichia anomala* MTCC-237 were employed for testing. The inoculum was adjusted to approximately 5×10^5 CFU/mL with sterile saline solution. Samples were prepared at a concentration ranging from 200 to 800µg in designated wells. Mueller-Hinton agar was used for bacterial culture, while Czapek 's-Dox agar was employed for fungal culture. Incubation for bacteria was carried out at 37 ℃ for 72 hours, and at 28 ℃ for fungi. Subsequently, the diameters of the inhibition zones (mm) were meticulously measured.

Antioxidant Activities

The radical-scavenging capabilities of the samples were investigated using stable DPPH radical as outlined by Blois (1958).[24-26] Varying concentrations (0 to 100 µg/mL) of samples and 2 mL of DPPH (100µM) were combined, brought to a total volume of 3 mL with methanol, and incubated in darkness for 45 minutes at room temperature. Following the incubation period, absorbance was measured using a spectrophotometer (Shimadzu UV-1800, Kyoto, Japan) at 517 nm against a blank (without sample/ standard). The free radical scavenging capacity of samples was calculated and expressed in IC_{50} values in comparison with BHT as a standard antioxidant.

RESULTS AND DISCUSSION

Chemistry

Newly synthesized Schiff base ligand and its metal complexes exhibited remarkable stability at ambient temperature and demonstrated solubility in various solvents, including ethanol, methanol, DMF, chloroform, and DMSO. The molar conductivity measured in DMF solvent showed that the synthesized complexes are non-electrolytes. The elemental analysis results were in accordance with the calculated values and are presented in Table-1.

Table-1: Physical Properties and analytical data of CIA and its metal complexes

Compounds	Colour	Mol.Wt	Yield (%)	CHN values (%) (calculated)				Molar Conductance ($ohm^{-1}cm^{-2}mol^{-1}$)	Melting Point (℃)
				M	C	H	N		
CIA	Dune	255.70	70	-	65.76 (65.26)	3.94 (3.81)	16.43 (16.27)	-	197
$[Co(CIA)_2Cl_2]$	Mint	641.24	66	9.19 (9.04)	52.44 (52.23)	3.14 (3.05)	13.11 (12.96)	23	241

$[Ni(CIA)_2Cl_2]$	Mustard	641.00	68	9.16 (9.07)	52.46 (52.23)	3.14 (3.06)	13.11 (12.89)	19	235
$[Cu(CIA)_2Cl_2]$	Emerald Green	645.85	65	9.84 (9.67)	52.07 (51.87)	3.12 (3.03)	13.01 (12.77)	21	243

^{1}H NMR and ^{13}C NMR

In the ^{1}H NMR spectra of CIA, the aromatic protons were observed as multiples within the range of 6.19 to 8.28 ppm. A distinct singlet was noted at 9.93 ppm corresponding to the CH=N. Another sharp signal appeared at 12.14 ppm, indicating the presence of an aromatic NH. The ^{13}C NMR spectra of CIA revealed thirteen distinct carbon environments, with chemical shifts ranging from 109.30 to 158.53 ppm. The alkene group resonance was observed at 158.53 ppm. The remaining carbons of the benzene ring, aldehyde, and pyridine ring appeared in the range 109.30 - 145.66 ppm.

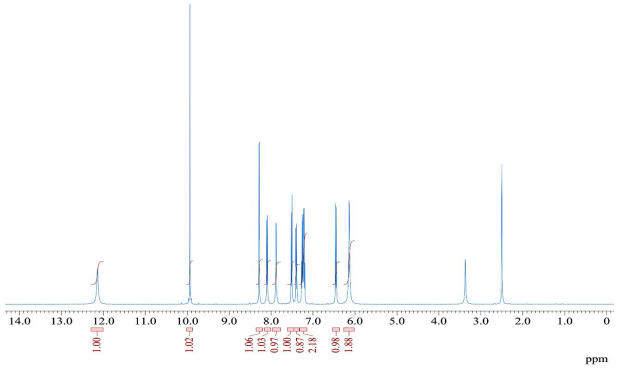

Fig.-1: ^{1}H NMR Spectrum of CIA

Mass Spectral Studies

Mass spectrometric analysis confirmed the proposed formulas of the synthesized ligand, which are shown in Fig.-2. The ligand (CIA) exhibited a peak at m/z 256.06, corresponding to its molecular mass. The mass spectra were also recorded for Co(II), Ni(II), and Cu(II) complexes, which displayed molecular ion peaks at m/z 641.24, 641.00, and 645.85, respectively, indicating 1:2 metal-to-ligand stoichiometry. These results align with the proposed molecular structures.

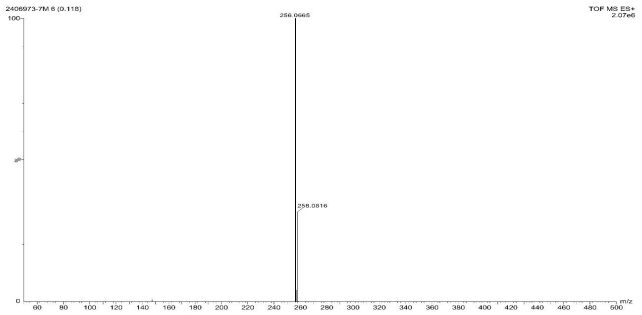

Fig.-2: Mass Spectrum of CIA

IR Spectral Studies

Infrared spectroscopy is an essential technique for identifying functional groups in synthesized ligands (CIA) and their metal complexes. The IR spectra of CIA and its metal complexes were recorded using KBr pellets in the range of 4000-350 cm^{-1}. In the IR spectrum of CIA, the position of ν(−NH) stretching was observed at 3168 cm^{-1}. The ν(C=N) uncoordinated ligand appeared at 1627 cm^{-1}, which is shifted by 10-20 cm^{-1}in their metal complexes, indicating that the coordination of the ligand to the metal occurs through the N-atom. In addition, new bands appeared in the region of 419-434 cm^{-1}indicates participation of the ligand in the formation of the complex with the metal. The IR spectra of both CIA and its metal complexes are provided in Fig.-3.

Table-2: FT-IR Spectral Data (cm^{-1}) of CIA and its Metal Complexes

Compounds	ν(NH)	ν(C=N)	ν(M−N)
CIA	3168	1627	-
$[Co(CIA)_2Cl_2]$	3190	1634	419
$[Ni(CIA)_2Cl_2]$	3197	1641	427
$[Cu(CIA)_2Cl_2]$	3176	1649	434

Electronic Spectra and Magnetic Moment Studies

The electronic spectra and magnetic moment studies of the CIA and its metal complexes were conducted, and the results are presented in Table-3, and the spectra are shown in Fig.-4. CIA exhibited an absorption band at 34,014 cm^{-1} due to a charge transfer transition. The $[Co(CIA)_2Cl_2]$ showed two bands at 14,836 and 16,474 cm^{-1} for the $^4T_1g(F) \rightarrow {}^4T_2g(F)$ and $^4A_2g(F) \rightarrow {}^4A_2g(F)$ transitions respectively.

The observed magnetic moment of $[Co(CIA)_2Cl_2]$ was 3.75 BM, and the electronic transitions suggest an octahedral geometry. The $[Ni(CIA)_2Cl_2]$ exhibited three bands at 12,594, 15,015 and 23,923 cm^{-1}, which are assigned to $^3A_2g(F) \rightarrow {}^3T_2g(F)$, $^3A_2g(F) \rightarrow {}^3T_1g(F)$ and $^3A_2g(F) \rightarrow {}^3T_1g(P)$ transitions respectively. Further, the magnetic moment of 2.88 BM and its electronic transitions suggest an octahedral geometry. Similarly, a broad band of $[Cu(CIA)_2Cl_2]$ appeared at 11,494 cm^{-1}, assigned to the $^2Eg \rightarrow {}^2T_2g$ transition with a shoulder at 10,989 cm^{-1}, and in addition, the magnet moment of 1.75 BM suggests an octahedral geometry.

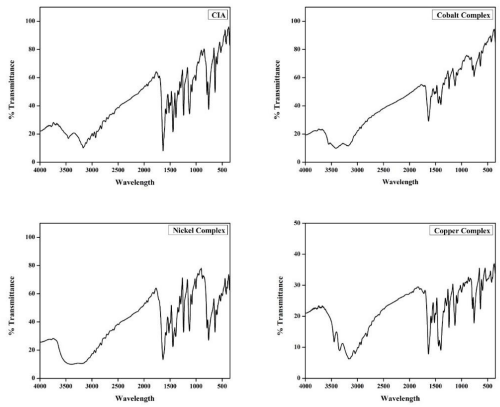

Fig.-3: FT-IR Spectra of CIA and its Metal Complexes

Table-3: Electronic Absorption Spectral Bands and Magnetic Moment Values of Synthesized Compounds

Compounds	λ (cm^{-1})	Electronic Transitions	Magnetic Moment (BM)
CIA	34,014	-	-
$[Co(CIA)_2Cl_2]$	14,836 16,474	$^4T_1g(F) \rightarrow {}^4T_2g(F)$ $^4A_2g(F) \rightarrow {}^4A_2g(F)$	3.75
$[Ni(CIA)_2Cl_2]$	12,594 15,015 23,923	$^3A_2g(F) \rightarrow {}^3T_2g(F)$ $^3A_2g(F) \rightarrow {}^3T_1g(F)$ $^3A_2g(F) \rightarrow {}^3T_1g(P)$	2.88
$[Cu(CIA)_2Cl_2]$	11,494 10,989	$^2Eg \rightarrow {}^2T_2g$ Shoulder	1.75

X-ray Diffraction Analysis

The X-ray diffraction analysis was performed on the synthesized metal complexes to assess their degree of crystallinity. The samples were scanned at a rate of 10 degrees per minute within a 5–90 degree range using a constant wavelength of 154 Å. The interplanar distance (d) was calculated using Bragg's formula $n\lambda=2dSin\theta$. The diffractogram revealed distinct peaks for the Co(II) complex with a relative intensity of 2θ reflections. The corresponding hkl values of 1,1, 4, and 4 are consistent with a cubic crystal structure.

The Ni(II) complex exhibited maximum intensities for 5 reflections with h, k, l values of 1, 1, 2, 3, and 4. Similarly, the Cu(II) complex displayed h, k, l values of 1, 1, 4, 4, and 5, indicating a cubic crystal structure.

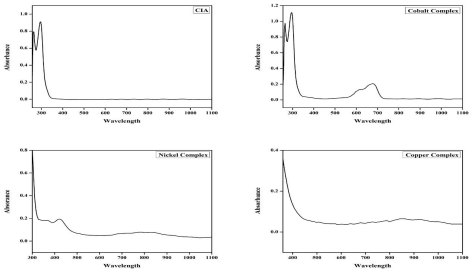

Fig.-4: Electronic Absorption Spectra of CIA and its Metal Complexes

The values are summarized in Table-4, and the corresponding diffraction patterns are presented in Fig.-5. All the synthesized metal complexes exhibited a crystalline nature, characterized by the regular arrangement of molecules. This structural property influences potential applications of transition metal complexes of CIA in various fields.[27]

Table-4: XRD Spectral Data of Synthesized Complexes

Compound	Point	2θ (degree)	Sinθ	$Sin^2θ$	$Sin^2θ×1000$	$h^2+k^2+l^2$	h k l	D		a in Å
								Obs	Cal	
$[Co(CIA)_2Cl_2]$	1	15.6	0.135	0.0182	18.22	1	1 0 0	5.70	5.78	5.70
	2	16.2	0.14	0.0196	19.6	1	1 0 0	5.49	5.53	5.49
	3	30.8	0.278	0.0676	67.6	4	2 0 0	2.96	3.01	5.92
	4	32.4	0.278	0.0772	77.2	4	2 0 0	2.76	2.81	5.53
$[Ni(CIA)_2Cl_2]$	1	14.9	0.129	0.0166	16.6	1	1 0 0	5.96	5.98	5.96
	2	16.53	0.143	0.0204	20.4	1	1 0 0	5.38	5.39	5.38
	3	19.3	0.167	0.0278	27.8	2	1 1 0	4.60	4.62	6.51
	4	25.2	0.218	0.0475	47.5	3	1 1 1	3.53	3.55	6.11
	5	30.6	0.263	0.0691	69.1	4	2 0 0	2.92	2.95	5.85
$[Cu(CIA)_2Cl_2]$	1	15.6	0.13	0.0169	16.9	1	1 0 0	5.92	5.96	5.92
	2	16.4	0.142	0.0201	20.1	1	1 0 0	5.42	5.39	5.42
	3	28.3	0.244	0.0595	59.5	4	2 0 0	3.15	3.18	6.30
	4	30.5	0.263	0.0691	69.1	4	2 0 0	2.92	2.98	5.85
	5	32.6	0.28	0.0784	78.4	5	2 1 0	2.74	2.76	6.14

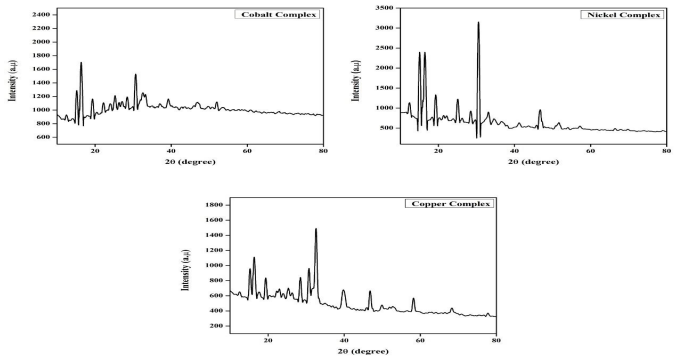

Fig.-5: Power XRD of CIA and its Metal Complexes

Scanning Electron Microscope (SEM)

The Scanning Electron Microscope (SEM) results for ligand CIA and its metal complexes are presented in Fig.-6. These studies provide valuable insights into the morphological structures of synthesized compounds. In the SEM images of CIA, the structure exhibits a broken stone shape, while the structure observed for $[Co(CIA)_2Cl_2]$ is a Kitchen sponge in shape. The $[Ni(CIA)_2Cl_2]$ appears to have a calcite-like structure, whereas $[Cu(CIA)_2Cl_2]$ exhibits an untreated maple wood floor-like structure.

Photocatalytic Studies

The Photodegradation capabilities of Co(II), Ni(II), and Cu(II) complexes were assessed through a series of controlled experiments involving natural sunlight exposure. In these experiments, the degradation of the EBT dye was carefully monitored by recording the absorbance at specific wavelengths 538.78, 542.80, and 546.44 nm, which correspond to the absorbance peaks of the dye when interacting with the metal complexes, indicating the ongoing photodegradation process. The UV-Visible spectra of the dye and metal complex mixtures were regularly recorded at 15-minute intervals, with the degradation period lasting up to 90 minutes. This allowed for a detailed assessment of the dye's breakdown over the time interval. A careful analysis of the spectral data showed that the photodegradation occurs and the dye degrades with amounts of 31.81, 35.29, and 67.44% by Co(II), Ni(II), and Cu(II) complexes, respectively.

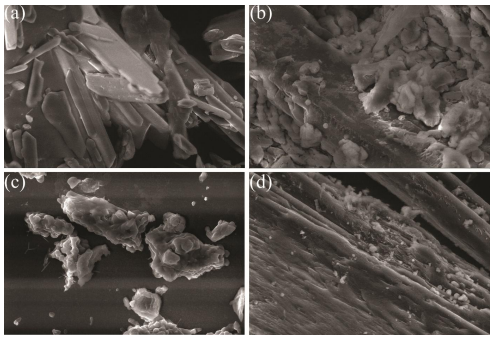

Fig.-6: SEM images of (a) CIA (b) $[Co(CIA)_2Cl_2]$ (c) $[Ni(CIA)_2Cl_2]$ and (d) $[Cu(CIA)_2Cl_2]$

The percentage degradation results suggest that the $[Cu(CIA)_2Cl_2]$ showed significantly higher photodegradation efficiency when compared to $[Co(CIA)_2Cl_2]$ and $[Ni(CIA)_2Cl_2]$. The higher degradation percentage for $[Cu(CIA)_2Cl_2]$ can be attributed to the catalytic properties of the metal complex, which may facilitate more efficient electron transfer along with light absorption and thereby enhancing the dye's degradation. In contrast, the $[Co(CIA)_2Cl_2]$ and $[Ni(CIA)_2Cl_2]$ were found to be less efficient and among these two metal complexes, $[Co(CIA)_2Cl_2]$ exhibited lower order of degradation efficiency of the synthesized metal complexes are represented as $[Cu(CIA)_2Cl_2]>[Ni(CIA)_2Cl_2]>[Co(CIA)_2Cl_2]$.[28]

The percentage of degradation was calculated by using the following equation:

$$\text{The percentage of degradation} = [(Co - Ct)/Co] \times 100$$

Where Co represents the initial concentration of the substance being studied. Ct represents the concentration of the compound being studied at time 't'. The photodegradation of EBT by all the metal complexes is calculated in percentage, and the values are compared with the literature values as shown in Table-5.

Table-5: Comparison of Results of Degradation of EBT Dye with Literature Values

Compound	Method of Analysis	% Of Photodegradation	References
Fe_3O_4@PVA-Au/ZnO	UV	51.4% 64.75%	29
NaN_3	UV	37%	30
$[Co(CIA)_2Cl_2]$	UV	31.81%	This Work
$[Ni(CIA)_2Cl_2]$		35.29%	This Work
$[Cu(CIA)_2Cl_2]$		67.44%	This Work

Results and Discussion of Biological Activities

Antimicrobial Activities

Synthesized ligand and its metal complexes were evaluated for their antimicrobial activities at concentrations from 200 to 800 µg/mL against two bacterial strains (*Staphylococcus aureus* and *Escherichia coli*) and two fungal strains (*A. flavous* and *P. anomala*). The results revealed that the metal complexes exhibited superior activity compared to the uncoordinated ligand. The metal complex of

the ligand, $[Cu(CIA)_2Cl_2]$ shows significant activity against both bacterial and fungal strains. While the other two metal complexes were also found to have better activity, they were quite lower when compared to the $[Cu(CIA)_2Cl_2]$. The higher antimicrobial activity of the metal complexes can be attributed to the chelation theory, which suggests that metal ions enhance the stability. Additionally, the overtones concept relates to the increased permeability of the cell membrane due to the larger molecular size of metal complexes.

However, it is crucial to acknowledge that the biological activity of the ligand and its complexes was inferior when compared to Kanamycin, a standard for antibacterial activity, and Fluconazole, a standard used for antifungal activity.[31] The antibacterial and antifungal activity of the synthesized metal complexes is compared and graphically represented in Fig.-8 and 9, respectively.

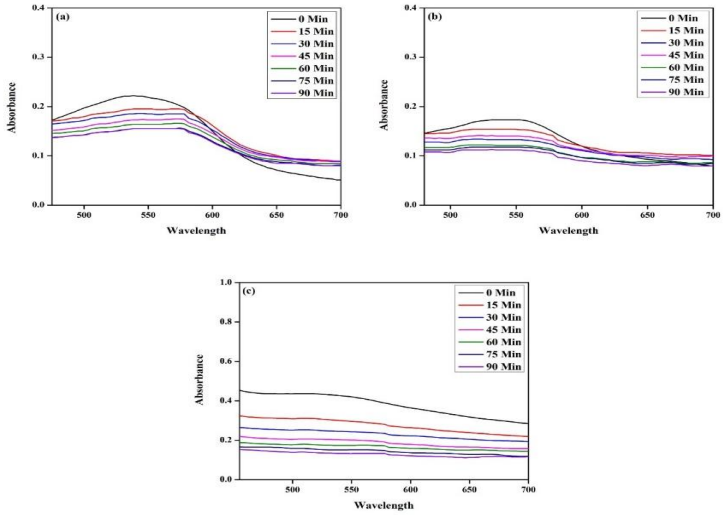

Fig.-7: Absorbance Spectra of Photocatalytic Degradation of EBT Dye in the Presence of (a) $[Co(CIA)_2Cl_2]$, (b) $[Ni(CIA)_2Cl_2]$, and (c) $[Cu(CIA)_2Cl_2]$

Table-6: Antibacterial Activity of CIA and its Metal Complexes

S. No.	Sample Name	Conc. (µg)	*Staphylococcus aureus*	*Escherichia coli*
1	CIA	200	3.66 ± 0.57	2.33 ± 0.57
		400	4.33 ± 0.57	3.66 ± 0.57
		600	6.33 ± 0.57	5.33 ± 0.57
		800	7.33 ± 0.57	6.66 ± 0.57
2	$[Co(CIA)_2Cl_2]$	200	4.33 ± 0.57	3.66 ± 0.57
		400	5.66 ± 0.57	4.33 ± 0.57
		600	6.66 ± 1.15	5.33 ± 0.57
		800	8.66 ± 0.57	7.33 ± 0.57
3	$[Ni(CIA)_2Cl_2]$	200	5.66 ± 0.57	4.33 ± 0.57
		400	6.33 ± 0.57	5.66 ± 0.57
		600	7.66 ± 0.57	6.33 ± 0.57
		800	9.33 ± 0.57	8.66 ± 0.57
4	$[Cu(CIA)_2Cl_2]$	200	7.66 ± 0.57	8.33 ± 0.57
		400	9.66 ± 0.57	10.33 ± 0.57
		600	11.66 ± 0.57	12.33 ± 0.57
		800	13.33 ± 0.57	13.66 ± 0.57
5	Kanamycin	20	9.33 ± 0.57	14.66 ± 0.57
		40	11.33 ± 0.57	15.66 ± 1.52
		60	13.66 ± 0.57	16.33 ± 0.57
		80	15.33 ± 0.57	17.66 ± 0.57

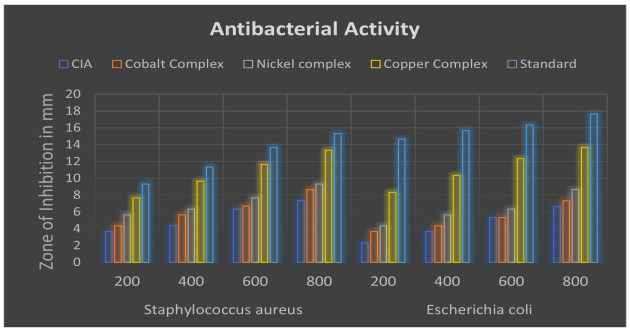

Fig.-8: Antibacterial Activity of CIA and its Metal Complexes

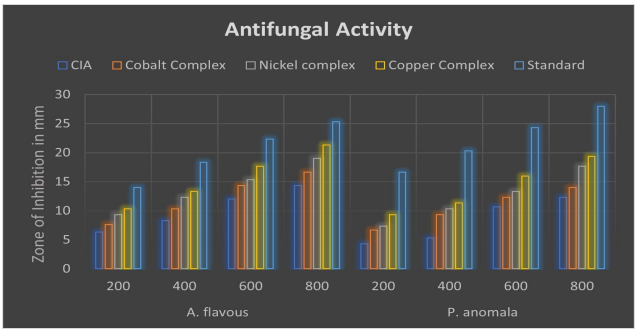

Fig.-9: Antifungal Activity of CIA and its Metal Complexes

Antioxidant Activity

The antioxidant activity of the synthesized CIA and its metal complexes was evaluated using the DPPH assay. The standard BHT was used as a reference, and the antioxidant activity was measured through IC_{50} values. Table-7 and Fig.-10 provide detailed information on the antioxidant activity of various compounds. The metal complexes exhibited good antioxidant activity by the DPPH assay method.[32, 33]

Table-7: Antifungal Activity of CIA and its Metal Complexes

S. No.	Sample Name	Conc. (µg)	*A. flavous*	*P. anomala*
1	CIA	200	6.33 ± 1.15	4.33 ± 1.15
		400	8.33 ± 1.15	5.33 ± 1.15
		600	12.00 ± 1.73	10.66 ± 1.15
		800	14.33 ± 1.15	12.33 ± 1.15
2	$[Co(CIA)_2Cl_2]$	200	7.66 ± 1.15	6.66 ± 1.15
		400	10.33 ± 1.15	9.33 ± 1.15
		600	14.33 ± 1.15	12.33 ± 1.15
		800	16.66 ± 1.15	14.00 ± 1.73
3	$[Ni(CIA)_2Cl_2]$	200	9.33 ± 1.15	7.33 ± 1.15
		400	12.33 ± 1.15	10.33 ± 1.15
		600	15.33 ± 1.15	13.33 ± 1.15
		800	19.00 ± 1.73	17.66 ± 1.15
4	$[Cu(CIA)_2Cl_2]$	200	10.33 ± 1.15	9.33 ± 1.15
		400	13.33 ± 1.15	11.33 ± 1.15
		600	17.66 ± 1.15	16.00 ± 1.73
		800	21.33 ± 1.15	19.33 ± 1.15
5	Fluconazole	100	14.00 ± 1.73	16.66 ± 1.15
		200	18.33 ± 1.15	20.33 ± 2.08
		300	22.33 ± 1.15	24.33 ± 1.15
		400	25.33 ± 1.15	28.00 ± 1.73

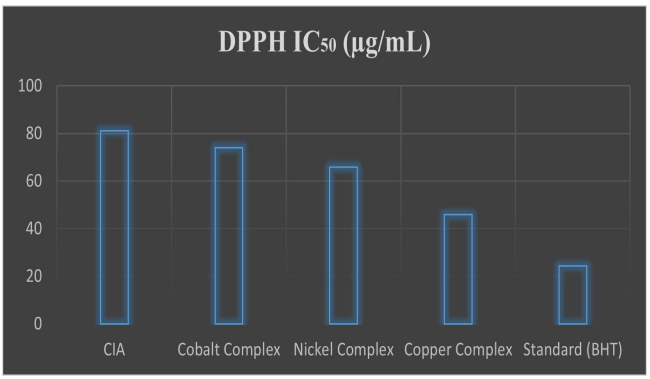

Fig.-10: Antioxidant Activity of CIA and its Metal Complexes

Table-8: Antioxidant Activity of CIA and its Metal Complexes

Sample Name	DPPH IC_{50} (µg/mL)
CIA	81.104
$[Co(CIA)_2Cl_2]$	73.980
$[Ni(CIA)_2Cl_2]$	65.773
$[Cu(CIA)_2Cl_2]$	45.874
Standard (BHT)	24.330

CONCLUSION

The present research focuses on the synthesis and evaluation of biologically active Co(II), Ni(II), and Cu(II) complexes of novel ligand 5-chloro-*N*-[(1*Z*)-1*H*-indol-3-ylmethylene]pyridin-2-amine (CIA). Various physicochemical and spectral methods were employed to characterize these compounds. X-ray data showed the crystalline nature of all synthesized metal complexes. SEM graphs show that the metal complexes have good surface properties by having different surface morphologies. The synthetic approach yielded complexes with a 1:2 metal to ligand molar ratio, exhibiting bidentate coordination behavior and octahedral geometry. The photocatalytic activity of the synthesized complexes was assessed using EBT dye. With 67.44% degradation efficiency, Cu(II) complex exhibited the highest percentage of degradation when compared to Co(II) and Ni(II) complexes. The obtained results of antimicrobial, antifungal, and antioxidant activity suggest that $[Cu(CIA)_2Cl_2]$ exhibited fairly good activity.

ACKNOWLEDGMENTS

Authors are thankful to Sahyadri Science College, Kuvempu University, Shivamogga, for providing the facility, and Mangalore University for providing the spectral analysis.

CONFLICT OF INTERESTS

The authors declare that there is no conflict of interest.

AUTHOR CONTRIBUTIONS

The present work is related to *SDG-6: Clean Water and Sanitation*. All the authors contributed significantly to this manuscript, participated in reviewing/editing and approved the final draft for publication. The research profile of the authors can be verified from their ORCID ids, given below:

G.Y. Akarsh http://orchid.org/0000-0002-3291-0709
H.A. Anilkumara http://orchid.org/0000-0002-1009-0797
N.K. Vasantakumarnaik http://orchid.org/0000-0001-6794-7651
N. Ranjitha http://orchid.org/0000-0002-1444-0969
G. Suma http://orchid.org/0000-0001-7623-3343
K.M. Pooja http://orchid.org/0000-0001-7623-3343
G. Krishnamurthy http://orchid.org/0000-0002-5292-7858

REFERENCES

1. N Ranjitha, G Krishnamurthy, H S Bhojya Naik, Malathesh Pari, Lubna Afroz, K R Sumadevi, and M N Manjunatha, *Inorganica Chimica Acta*, **543**, 121191(2022), https://doi.org/10.1016/j.ica.2022.121191
2. H.A. Anilkumara, G. Krishnamurthy, M.N. Manjunatha, Malathesh Pari, N. Ranjitha, R.S. Priya Rani, and G.Y. Akarsh, *Journal of Molecular Structure*, **1315**, 138752(2024), https://doi.org/10.1016/j.molstruc.2024.138752
3. N.K. Vasantakumarnaik, G. Krishnamurthy, Malathesh Pari, N. Ranjitha, H.A. Anilkumara, G.Y. Akarsh and M.N. Manjunatha, *Journal of Molecular Structure*, **1294**, 136405(2023), https://doi.org/10.1016/j.molstruc.2023.136405
4. N. Ranjitha, G. Krishanamurthy, M.N. Manjunath, H. S. Bhojya Naik, Malathesh Pari, N. K. Vasanthkumarnaik, J. Lakshmikantha, and K. Pradeep, *Journal of Molecular Structure*, **1274**, 134483(2023), https://doi.org/10.1016/j.molstruc.2022.134483
5. U. Agarwal, N.P. Singh, A. Kumar and K. Kumar, *Rasayan Journal of Chemistry,* **13***,* 1685(2020), http://dx.doi.org/10.31788/RJC.2020.1335689
6. Aysegul Golcu, Mehmet Tumer, Havva Demirelli, and R. Alan Wheatley, *Inorganica Chimica Acta*, **358**, 1785(2005), https://doi.org/10.1016/j.ica.2004.11.026
7. N. P. Singh, K. Kumar, A. Kumar, and U. Agarwal, *Rasayan Journal of Chemistry*, **13**, 215(2020), http://dx.doi.org/10.31788/RJC.2020.1315571
8. Yi Jia and Junbai Li, *Chemical Reviews*, **115** 1597(2015), https://doi.org/10.1021/cr400559g
9. Kistan, V. Kanchana, C. Esther Jeyanthi, and K. Uma, *Rasayan Journal of Chemistry,* **16**, 2171(2023), http://doi.org/10.31788/RJC.2023.1648523
10. L. Cottet, C. A. P. Almeida, N. Naidek, M. F. Viante, M. C. Lopes, and N. A. Debacher, *Applied Clay Science*, **95**, 25(2014), https://doi.org/10.1016/j.clay.2014.03.023
11. J. Khalid AL-Adilee, K. Ahmed Abass, and M. Taher *Journal of Molecular Structure*, **1108**, 378(2016), https://doi.org/10.1016/j.molstruc.2015.11.038
12. J. Lesy Josephine, A. Mathunika Devi, K. Thanigaimani1 and P. Ramanathan, *Rasayan Journal of Chemistry*, **16**, 721(2023), http://doi.org/10.31788/RJC.2023.1628161
13. Oliver Gutfleisch, Matthew A. Willard, Ekkes Brück, Christina H. Chen, S. G. Sankar and J. Ping Liu, *Advanced Materials*, **23**, 821(2011), https://doi.org/10.1002/adma.201002180
14. Peter A. Lieberzeit and Franz L. Dickert, *Analytical and Bioanalytical Chemistry*, **387**, 237(2006), https://doi.org/10.1007/s00216-006-0926-z
15. Muhammet Köse, Savas Purtas, Seyit Ali Güngör, Gökhan Ceyhan, Eyup Akgün, and Vickie McKee, *Spectrochimica Acta Part A: Molecular and Biomolecular Spectroscopy*, **136**, 1388(2015), https://doi.org/10.1016/j.saa.2014.10.025
16. Haoqi Yang, Jiyoung Lee, Jun Young Cheong, Yifan Wang, Gaigai Duan, Haoqing Hou, Shaohua Jiang, and Il-Doo Kim, *Energy & Environmental Science*, **14**, 4228(2021), https://doi.org/10.1039/D1EE00419K
17. John J. Shea and Chao Luo, *ACS Applied Materials & Interfaces*, **12**, 5361(2020), https://doi.org/10.1021/acsami.9b20384
18. N.K. Vasantakumarnaik, G. Krishnamurthy, Malathesh Pari, N.Sunil Kumar, N. Venugopal, and T. Manjuraj, *Journal of Molecular Structure*, **1332**, 14016(2025), https://doi.org/10.1016/j.molstruc.2024.140461
19. N. Venugopal, G. Krishnamurthy, H.S. Bhojyanaik and M. Giridhar, *Journal of Molecular Structure*, **1191** ,85(2019), https://doi.org/10.1016/j.molstruc.2019.04.022
20. G.Y. Akarsh, M.N. Manjunatha, B.S. Krishna, H.A. Anilkumara, N. Ranjitha, N.K. Vasantakumarna

ik and G. Krishnamurthy, *Journal of Molecular Structure*, **1332**, 140448(2025), https://doi.org/10.1016/j.molstruc.2024.140448
21. R.T.P. Pinto, M.R. Wolf-Maciel and L. Lintomen, *Computers & Chemical Engineering*, **24**, 1689(2000), https://doi.org/10.1016/S0098-1354(00)00455-5
22. Ehab M. Zayed, Gehad G. Mohamed, Ahmed M. M. Hindy, and J. Therm, *Journal of Thermal Analysis and Calorimetry*, **120**, 893(2014), https://doi.org/10.1007/s10973-014-4061-3
23. R. Champa, K.A. Vishnumurthy, Yadav D. Bodke, H.S. Bhojya Naik, Itte Pushpavathi, P. Meghana, and Priya R. Kadam, *Results in Chemistry*, **6**, 101018(2023), https://doi.org/10.1016/j.rechem.2023.101018
24. N. Raman, J. Dhaveethu Raja, and A. Sakthivel, *Chemical Science*, **119**, 303(2007), https://doi.org/10.1007/s12039-007-0041-5
25. Marsden S. Blois, *Nature*, **181**, 1199(1958), https://doi.org/10.1038/1811199a0
26. Nevin Turan and Kenan Buldurun, *European Journal of Chemistry*, **9**, 22(2018), https://doi.org/10.5155/eurjchem.9.1.22-29.1671
27. M.I. Khan, Ayub Khan, Iqbal Hussain, Murad Ali Khan, Saima Gul, Mohammad Iqbal, Inayat-Ur-Rahman, and Fazli Khuda, I*norganic Chemistry Communications*, **35**, 104(2013), https://doi.org/10.1016/j.inoche.2013.06.014
28. Vishnu G, Simranjeet Singh, T.S. Sunil Kumar Naik, R Viswanath, Praveen C. Ramamurthy, Pooja Bhadrecha, HS Bhojya Naik, Joginder Singh, Nadeem A. Khan and Sasan Zahmatkesh, *Journal of Cleaner Production*, **404**, 136977(2023), https://doi.org/10.1016/j.jclepro.2023.136977
29. Mohadeseh Forouzandeh-Malati, Fatemeh Ganjali, Elnaz Zamiri, Simindokht Zarei-Shokat, Farinaz Jalali, Mohsen Padervand, Reza Taheri-Ledari, and Ali Maleki, *Langmuir*, **38**, 45(2022), https://doi.org/10.1021/acs.langmuir.2c01822
30. Saeid Taghavi Fardood, Farzaneh Moradnia, Fateme Yekke Zare, Siamak Heidarzadeh, Mohammad Azad Majedi, Ali Ramazani, Mika Sillanpaa, and Ky Nguyen, *Scientific Reports*, **14**, 6755(2024), https://doi.org/10.1038/s41598-024-56666-2
31. N. Venugopal, G. Krishnamurthy, H. S. Bhojya Naik and J. D. Manohara, *Journal of Inorganic and Organometallic Polymers and Materials*, **30**, 2608(2020), https://doi.org/10.1007/s10904-019-01394-8
32. Wageeh A. Yehye, Noorsaadah Abdul Rahman, Azhar Ariffin, Sharifah Bee Abd Hamid, Abeer A. Alhadi, Farkaad A. Kadir, and Marzieh Yaeghoobi, *European Journal of Medicinal Chemistry*, **101**, 295(2015), https://doi.org/10.1016/j.ejmech.2015.06.026
33. V. Bondet, W. Brand-Williams and C. Berset, *Food Science and Technology*, **30**, 609(1997), https://doi.org/10.1006/fstl.1997.0240

[RJC-9359/2025]